

Momentum-based gradient descent methods for Lie groups

Cédric M. Campos

CEDRIC.MCAMPOS@URJC.ES

*Departamento de Matemática Aplicada, Ciencia e Ingeniería
de los Materiales y Tecnología Electrónica
Universidad Rey Juan Carlos
Calle Tulipán s/n, 28933 Móstoles, Spain*

David Martín de Diego

DAVID.MARTIN@ICMAT.ES

*Instituto de Ciencias Matemáticas (CSIC-UAM-UC3M-UCM)
Calle Nicolás Cabrera 13-15, 28049 Madrid, Spain*

Jose Torrente Teruel

JOSE.TORRENTETERUEL@GMAIL.COM

*Departamento de Matemáticas
Universidad de Córdoba
Edificio Albert Einstein, Campus de Rabanales, 14071 Córdoba, Spain*

Abstract

Polyak’s Heavy Ball (PHB; Polyak, 1964), a.k.a. Classical Momentum, and Nesterov’s Accelerated Gradient (NAG; Nesterov, 1983) are well know examples of momentum-descent methods for optimization. While the latter outperforms the former, solely generalizations of PHB-like methods to nonlinear spaces have been described in the literature. We propose here a generalization of NAG-like methods for Lie group optimization based on the variational one-to-one correspondence between classical and accelerated momentum methods (Campos et al., 2023). Numerical experiments are shown.

Keywords: Polyak’s heavy ball, Nesterov’s accelerated gradient, gradient descent, momentum methods, variational integrators, Lie groups

1. Introduction

A fundamental step of many of the recent advances in machine learning and data analysis consists of the minimization of a loss function. This loss function allows us to evaluate, for instance, how well the machine learning algorithm models the featured data set. Due to the typically large size of data, low-cost optimization techniques such as the gradient descent (GD) method are more convenient than methods that require the computation of second-order derivatives, like Newton’s method. Therefore, it is useful to accelerate gradient descent without increasing computational cost (Nesterov, 2004). Polyak (1964) introduced Classical Momentum (CM), also known as Polyak’s Heavy Ball (PHB), as a technique to accelerate gradient descent by taking into account previous gradients in the update rule at each iteration of the method. This is widely used in machine learning literature. Later, Nesterov (1983) found Nesterov’s Accelerated Gradient (NAG) method as an alternative optimization technique with an optimal convergence rate for the class of convex loss functions with Lipschitz gradient. All of these families of accelerated optimization methods have become popular in the machine learning community.

Given a convex function $f \in \mathcal{C}^2(\mathbb{R}^d, \mathbb{R})$ and the corresponding minimization problem

$$\arg \min_{x \in \mathbb{R}^d} f(x),$$

observe that the different convergence behavior of GD and accelerated optimization is retained in the continuous limit of these methods (Su et al., 2016):

$$\dot{x} + \nabla f(x) = 0, \tag{GD}$$

$$\ddot{x} + \frac{3}{t}\dot{x} + \nabla f(x) = 0. \tag{PHB/NAG}$$

GD is modeled by a first-order differential equation, while the continuous limit of accelerated methods such as PHB and NAG consists of a second-order differential equation (SODE). This SODE can be recovered from a variational principle as the Euler-Lagrange equations for the time-dependent Lagrangian (Wibisono et al., 2016)

$$L(t, x, \dot{x}) = t^3 \left(\frac{1}{2} \|\dot{x}\|^2 - f(x) \right).$$

Moreover, a force must be included to obtain the NAG method, hence modifying the SODE (Campos et al., 2023). The simulation of Lagrangian or Hamiltonian systems has made it possible to introduce discrete variational (Marsden and West, 2001) and symplectic methods (Sanz-Serna and Calvo, 1994; Hairer et al., 2010; Blanes and Casas, 2016) as a sub-product of the classical accelerated optimization methods. In particular, Campos et al. (2023) introduced variational integrators which allowed to generalize PHB and NAG, deriving two families of optimization methods in one-to-one correspondence. However, since the systems considered are explicitly time-dependent, the preservation of symplecticity occurs solely on the fibers.

In the majority of machine learning applications, the function to be optimized is modeled on a Euclidean space but other cases are also of considerable interest (see the work by Duruisseaux and Leok, 2022, 2023b, and references therein). Particularly, in this paper we study optimization problems where the objective function is defined on a Lie group (Absil et al., 2008) as in signal or image processing, independent component analysis (ICA), learning robotic systems etc (see Bernardini and Rinaldo (2021); Tao and Ohsawa (2020); Duruisseaux and Leok (2023a) and references therein). Such problems are usually tackled using similar techniques as in the standard Euclidean case, using, for instance, a constrained optimization procedure or an appropriate parametrization to transform them into unconstrained problems. Such algorithms are characterized by a reduced convergence due to the lack of a geometric framework. In this paper, we adopt an intrinsic point of view, constructing the accelerated methods on Lie groups using its inherent geometry.

The paper is organized as follows. In Section 2, we introduce the notation to be used in the following and give schematically the algorithms developed in this work. In fact, PHB and NAG methods in Lie groups can be computed using Algorithm 2. Section 3 is devoted to the derivation of both method families, Eqs. (3.6), using a discrete variational perspective from a forced discrete Lagrangian system on a Lie group. We also give an alternative derivation from a Hamilton-Pontryagin variational principle. In the remaining two sections are devoted to exemplify the methods and test the computational performance of the optimization

techniques with respect to the Gradient Descent method. Several objective functions are defined, and explicit solvers for these (*a priori* implicit) methods are presented in section 4. They involve two important retraction maps: the exponential map and the Cayley transform. Then, section 5 give numerical simulations to the test functions. The algorithms introduced here are generally shown to be improvements over Gradient Descent, except discrepancy in some cases. Conclusions and overall discussion can be found in section 6. Finally, to make the paper self-contained, we have included at the end some appendices with the necessary technical results on Lie groups that we have used along the work.

2. The methods

2.1 Notation

- G denotes a Lie group, the associated Lie algebra is $\mathfrak{g} = T_e G$, and \mathfrak{g}^* its dual.
- L_g and R_h are the left and right actions of the group, $L_g(h) = gh = R_h(g)$. Their tangent maps at the identity, $T_e L_g$ and $T_e R_h$, are still denoted L_g and R_h .
- Given a real-valued function $\phi: G \rightarrow \mathbb{R}$, $d\phi: TG \rightarrow \mathbb{R}$ is the differential of ϕ , a 1-form over G .
- $(\cdot)^*$ denotes the pullback.
- We consider an inner product $\langle \cdot, \cdot \rangle$ on \mathfrak{g} , for which $(\cdot)^b: \mathfrak{g} \rightarrow \mathfrak{g}^*$ and $(\cdot)^\sharp: \mathfrak{g}^* \rightarrow \mathfrak{g}$ denote the musical operators, and $(\cdot)^t$ the transposition of linear maps.
- $\nabla\phi$ is the right-trivialized gradient, $\nabla\phi(g) := (\mathbf{R}_g^* d\phi(g))^\sharp$.
- $\tau: \mathfrak{g} \rightarrow G$ is a retraction map, and $d\tau_\xi: \mathfrak{g} \rightarrow \mathfrak{g}$, for $\xi \in \mathfrak{g}$, denotes its right-trivialized tangent (see Appendix A).
- Δ is the forward difference operator. For vectors (and covectors), it is the standard operator, *e.g.* $\Delta[\omega_0] = \omega_1 - \omega_0$, either in \mathfrak{g} or in \mathfrak{g}^* . For group elements, it gives the right-transition, $\Delta w_0 = w_0^{-1} w_1$ in G , an “arrow” joining w_0 with w_1 when acting on the right of w_0 : $\mathbf{R}_{\Delta w_0}(w_0) = w_0 \Delta w_0 = w_1$.

2.2 Momentum-Descent Methods for Lie groups

Given a Lie group G , let $\phi: D \subseteq G \rightarrow \mathbb{R}$ denote a real-valued \mathcal{C}^1 -function defined on a path-connected open subset $D \subseteq G$. Assume that ϕ possesses a single local minimum in D ,

$$g^* = \operatorname{argmin}_{g \in D} \phi(g).$$

To seek for g^* , we propose a family of twin methods inspired in the one-to-one correspondence between PHB and NAG methods (Campos et al., 2023). In fact, they are equivalent to “regular” PHB and NAG when $G = \mathbb{R}^n$. For further details, see Section 3. This correspondence allows for the compilation of both in a single algorithm, Algorithm 1, with a Boolean input or hyperparameter to set the family of choice: $\epsilon = 0$, PHB-like method;

```

00 input:  $\nabla\phi: G \rightarrow \mathfrak{g}$ ,  $g_0 \in G$ ;  $\varepsilon \in \{0,1\}$ ,  $\mu, \eta: \mathbb{N}_0 \rightarrow \mathbb{R}$ 
01  $g_1 \leftarrow g_0$ ,  $x_0 \leftarrow 0$ ,  $x_1 \leftarrow 0$ ,  $y_1 \leftarrow -\eta_0 \nabla\phi(g_0)$ ,  $z_1 \leftarrow \varepsilon y_1$ 
02 for  $k = 1$  to  $N - 1$ 
03      $y_{k+1} \leftarrow x_k - \eta_k \nabla\phi(g_k)$ 
04      $z_{k+1} \leftarrow (1 - \varepsilon)x_k + \varepsilon y_{k+1}$ 
05      $x_{k+1} \leftarrow y_{k+1} + \mu_k \Delta z_k$ 
06      $g_{k+1} \leftarrow g_k \tau(\xi_k)$  such that  $\xi_k = d\tau_{\xi_k}^t (\text{Ad}_{g_k}^t \Delta x_k)$ 
07 end for
08 output:  $g_N$ 

```

Algorithm 1: Momentum-Descent method for Lie groups. Minimizes ϕ from the initial guess g_0 . Set $\varepsilon = 0$ for PHB, or $\varepsilon = 1$ for NAG.

$\varepsilon = 1$, NAG-like method. A further hyperparameter is the strategy, a couple of discrete-time dependent coefficients, (μ_k, η_k) . μ_k is usually referred to as the momentum coefficient and η_k as the learning rate.

Inputs are given on line 00, namely, $\nabla\phi$, the right trivialized gradient of the objective function, and g_0 , an initial guess for the argument minimum. At line 01, the direction search is set to a safe value (start still), besides of initializing some variables to the values given in (3.7). Starting on line 02 with $k = 1$, at line 03, a gradient descent step is taken, and then a momentum step at line 05, that gives a new momentum Δx_1 , which in turn is used at line 06 together with g_1 to compute a new approximation g_2 for g^* using the reconstruction equation (3.5b). This process is iterated along lines 02–07 following the dynamical equation (3.5a) in the form of (3.6). The last iterate, g_N , is then outputted.

The variable of interest is g , in fact, g_k is a trajectory of group elements towards g^* . x and y are auxiliary variables in \mathfrak{g} to carry part of the dynamics. The variable z on line 04 is a further auxiliary variable in \mathfrak{g} to set the family of choice through the Boolean hyperparameter ε . In a final implementation, according to the family choice, either the variable x or y should appear instead of z on line 05.

The computational load is concentrated in the gradient evaluation, line 03, one per iteration, and in the reconstruction step, line 06. Although it is implicit in general, it can be rendered explicit in some cases. For instance, when G is the Euclidean space \mathbb{R}^n , then $g_k = x_k$ and line 06 reduces to the tautological relation

$$x_{k+1} = x_k + \Delta x_k .$$

And more notably, when G is the group of rotations $SO(3)$ and τ is the matrix exponential, then $g_k = R_k$ and the aforementioned equation reads as in Equation (4.1a), that is,

$$R_{k+1} = \exp(\Delta x_k) R_k .$$

Finally, note that, for a strategy with null momentum, $\mu \equiv 0$, we recover gradient descent for Lie groups, Algorithm 2, which could be further simplified, but is left as is for easier comparison with Algorithm 1.

```

00 input:   $\nabla\phi: G \rightarrow \mathfrak{g}$ ,  $g_0 \in G$ ;  $\mu: \mathbb{N}_0 \rightarrow \mathbb{R}$ 
01  $x_0 \leftarrow 0$ 
02 for  $k = 0$  to  $N - 1$ 
03      $x_{k+1} \leftarrow x_k - \eta_k \nabla\phi(g_k)$ 
04      $g_{k+1} \leftarrow g_k \tau(\xi_k)$  such that  $\xi_k = d\tau_{\xi_k}^t (\text{Ad}_{g_k}^t \Delta x_k)$ 
05 end for
06 output:  $g_N$ 
    
```

Algorithm 2: Gradient Descent for Lie groups. Minimizes ϕ from the initial guess g_0 .

3. Development

Classical and accelerated momentum methods, *e.g.* Polyak’s Heavy Ball and Nesterov’s Accelerated Gradient, are equivalent to the discrete Euler-Lagrange equations of a particular discrete Lagrangian system (confer with Campos et al., 2023). For a \mathcal{C}^1 -function $\phi: D \subset \mathbb{R}^n \rightarrow \mathbb{R}$ these equations are

$$\Delta x_k = \mu_k \Delta [x_{k-1} - \varepsilon \eta_{k-1} \nabla\phi(x_{k-1})] - \eta_k \nabla\phi(x_k), \quad (3.1)$$

where Δ is the forward difference operator, μ_k and η_k are suitable coefficients (the method’s strategy), and ε is a boolean coefficient: $\varepsilon = 0$ for PHB and $\varepsilon = 1$ for NAG. The terms accompanying ε are associated to a force, hence NAG is in fact PHB with forces.

This equation may be split in two steps to determine x_{k+1} from x_k and x_{k-1} : a *gradient (descent)* step (3.2a), and a *momentum* step (3.2b):

$$y_{k+1} = x_k - \eta_k \nabla\phi(x_k), \quad (3.2a)$$

$$x_{k+1} = y_{k+1} + \mu_k \Delta z_k, \quad (3.2b)$$

where the variable z has a different meaning depending on the family of choice, $z \equiv x_{-1}$ for PHB, and $z \equiv y$ for NAG. Equation (3.2a) should be viewed as an auxiliary definition that transforms (3.1) into (3.2b) and vice versa. Although x ’s and y ’s follow a trajectory towards the argument minimum of ϕ , strictly speaking x_k is the natural one, referred here as “on track”, while we refer to y_k as the “off road” trajectory.

Consider now a real-valued \mathcal{C}^1 -function, ϕ , defined on a path-connected open subset D of a given Lie group G , that is, $\phi: D \subseteq G \rightarrow \mathbb{R}$. Assume furthermore that ϕ possess a single local minimum in D ,

$$g^* = \operatorname{argmin}_{g \in D} \phi(g). \quad (3.3)$$

We define on $D \times D \subset G \times G$ the discrete time-dependent Lagrangian system with forces (Marsden and West, 2001)

$$l_k(w_0, w_1) := a_k \frac{1}{2} \|\tau^{-1}(\Delta w_0)\|^2 - b_k^- \phi(w_0) - b_{k+1}^+ \phi(w_1), \quad (3.4a)$$

$$f_k^-(w_0, w_1) := -\frac{a_k - 1}{a_k} (b_k^- + b_k^+) d\phi(w_0), \quad (3.4b)$$

$$f_k^+(w_0, w_1) := (b_k^- + b_k^+) d\phi(w_0) \circ \mathbf{R}_{(\Delta w_0)^{-1}}, \quad (3.4c)$$

where $a_k > 0, b_k^\pm$ are arbitrary coefficients and $(w_0, w_1) \in D \times D$. The discrete Euler-Lagrange equations of a free/forced system are (Appendix F)

$$D_1 l_{k+1}(w_1, w_2) + D_2 l_k(w_0, w_1) + \varepsilon f_{k+1}^-(w_1, w_2) + \varepsilon f_k^+(w_0, w_1) = 0 \in \mathbb{T}_{w_1}^* G.$$

where, as earlier, ε is a boolean coefficient: $\varepsilon = 0$, free system; $\varepsilon = 1$, forced system. Taking into account that

$$\frac{\partial \tau^{-1}(\Delta w_0)}{\partial w_0} = -\mathbb{T}_{\Delta w_0} \tau^{-1} \circ \mathbb{L}_{w_0^{-1}} \circ \mathbb{R}_{\Delta w_0} \quad \text{and} \quad \frac{\partial \tau^{-1}(\Delta w_0)}{\partial w_1} = \mathbb{T}_{\Delta w_0} \tau^{-1} \circ \mathbb{L}_{w_0^{-1}},$$

we obtain in this particular case

$$\begin{aligned} & -a_{k+1} \mathbb{R}_{\Delta w_1}^* \mathbb{L}_{w_1^{-1}}^* (\mathbb{T}_{\Delta w_1} \tau^{-1})^* ((\tau^{-1}(\Delta w_1))^{\flat}) - b_{k+1}^- d\phi(w_1) \\ & + a_k \mathbb{L}_{w_0^{-1}}^* (\mathbb{T}_{\Delta w_0} \tau^{-1})^* ((\tau^{-1}(\Delta w_0))^{\flat}) - b_{k+1}^+ d\phi(w_1) \\ & - \varepsilon \frac{a_k}{a_{k+1}} (b_{k+1}^- + b_{k+1}^+) d\phi(w_1) + \varepsilon (b_k^- + b_k^+) \mathbb{R}_{(\Delta w_0)^{-1}}^* d\phi(w_0) = 0 \in \mathbb{T}_{w_1}^* G, \end{aligned}$$

where $(\cdot)^{\flat}$ is the musical flat operator. Divide by $-a_{k+1}$, reorder terms, pull back to the identity by the right action, and apply the musical sharp operator $(\cdot)^{\sharp}$ to get

$$\Delta x_{k+1} = \mu_{k+1} (\Delta x_k - \varepsilon \Delta [\eta_k \nabla \phi(w_0)]) - \eta_{k+1} \nabla \phi(w_1) \in \mathfrak{g}, \quad (3.5a)$$

where

$$\mu_k := \frac{a_{k-1}}{a_k}, \quad \eta_k := \frac{b_k^- + b_k^+}{a_k}, \quad \text{and} \quad \Delta x_k := \left(\mathbb{R}_{w_1}^* \mathbb{L}_{w_0^{-1}}^* (\mathbb{T}_{\Delta w_0} \tau^{-1})^* (\tau^{-1}(\Delta w_0))^{\flat} \right)^{\sharp}.$$

This last equation can be rewritten as

$$\Delta x_k = \left(d\tau_{\tau^{-1}(\Delta w_0)}^{-1} \circ \text{Ad}_{w_0^{-1}} \right)^t \tau^{-1}(\Delta w_0). \quad (3.5b)$$

Indeed,

$$\begin{aligned} \Delta x_k &= \left((\mathbb{T}_{\Delta w_0} \tau^{-1} \circ \mathbb{L}_{w_0^{-1}} \circ \mathbb{R}_{w_1})^* (\tau^{-1}(\Delta w_0))^{\flat} \right)^{\sharp} \\ &= \left(\mathbb{T}_{\Delta w_0} \tau^{-1} \circ \mathbb{L}_{w_0^{-1}} \circ \mathbb{R}_{w_1} \right)^t \tau^{-1}(\Delta w_0) \\ &= \left(d\tau_{\tau^{-1}(\Delta w_0)}^{-1} \circ \mathbb{R}_{(\Delta w_0)^{-1}} \circ \mathbb{L}_{w_0^{-1}} \circ \mathbb{R}_{w_1} \right)^t \tau^{-1}(\Delta w_0), \end{aligned}$$

where we have first used a simple relation between the musical operators, the dual map, and the map transpose, $(A^* v^{\flat})^{\sharp} = A^t v$, then the definition of τ 's right-trivialized tangent (A.1), and finally the commutativity of the left and right actions to get the adjoint representation after simplification.

The set of equations (3.5) defines two families of methods or a family of twin methods, to which we refer to as momentum methods for Lie groups: classical, when $\varepsilon = 0$; and accelerated, when $\varepsilon = 1$. Although (3.5a) is formally identical to (3.1), for the time being, it cannot be put in the form of (3.2): In (3.5) solely the bracketing Δ is the usual difference

operator, whereas Δw_k is the group right-transition, and Δx_k is merely a suggestive notation, that is, there is no canonical x_k and x_{k+1} such that $\Delta x_k = x_{k+1} - x_k$, which prevents to introduce (3.2a). However, if we set x_0 to any fixed value (for instance, $x_0 = 0 \in \mathfrak{g}$), then all $x_{k+1} = x_k + \Delta x_k$ become defined recursively.

We may now rewrite (3.5) for $w_j = g_{k+j}$ in the form of (3.2):

$$y_{k+1} = x_k - \eta_k \nabla \phi(g_k), \quad (3.6a)$$

$$z_{k+1} = (1 - \varepsilon)x_k + \varepsilon y_{k+1}, \quad (3.6b)$$

$$x_{k+1} = y_{k+1} + \mu_k \Delta z_k, \quad (3.6c)$$

$$g_{k+1} = g_k \Delta g_k \quad \text{such that} \quad \tau^{-1}(\Delta g_k) = d\tau_{\tau^{-1}(\Delta g_k)}^t (\text{Ad}_{g_k}^t \Delta x_k), \quad (3.6d)$$

where (3.6b) has been added for convenience, and where (3.6d) is the *reconstruction* step from Equation (3.5b). Note that this equation is implicit. In fact, $\xi_k := \tau^{-1}(\Delta g_k)$ is a solution of the fixed point equation $\xi = d\tau_{\xi}^t \eta$ with $\eta := \text{Ad}_{w_0}^t \Delta x_k$.

Being (3.5a) a difference equation of order 2, two initial values $g_0, g_1 \in G$ sufficiently closed to g^* are required. Given g_0 , take $g_1 = g_0$, for which (3.5b) gives $\Delta x_0 = 0 \in \mathfrak{g}$. Then define y_1 and z_1 using Equations (3.6a) and (3.6b) with $k = 0$, before running the whole scheme (3.6) for $k \geq 1$. In summary,

$$g_1 = g_0, \quad (x_0 = 0), \quad x_1 = x_0 + \Delta x_0, \quad y_1 = x_0 - \eta_0 \nabla \phi(g_0), \quad z_1 = (1 - \varepsilon)x_0 + \varepsilon y_0. \quad (3.7)$$

There is a workaround to avoid having to set x_0 : Subtract to consecutive sets of Eqs. (3.6) to get

$$\Delta y_{k+1} = \Delta x_k - \Delta[\eta_k \nabla \phi(g_k)], \quad (3.8a)$$

$$\Delta z_{k+1} = (1 - \varepsilon)\Delta x_k + \varepsilon \Delta y_{k+1}, \quad (3.8b)$$

$$\Delta x_{k+1} = \Delta y_{k+1} + \Delta[\mu_k \Delta z_k], \quad (3.8c)$$

$$g_{k+1} = g_k \Delta g_k \quad \text{such that} \quad \tau^{-1}(\Delta g_k) = d\tau_{\tau^{-1}(\Delta g_k)}^t (\text{Ad}_{g_k}^t \Delta x_k). \quad (3.8d)$$

Although this does not significantly increase the overall computational cost, its implementation would be slightly more cumbersome.

It is worth noting that in Eqs. (3.6) and (3.8), the trivialization has not been explicitly stated. The same choice, whether right or left trivialization, must be made in Eqs. (3.6a) and (3.6d).

Momentum based gradient descent methods for Lie groups such as Eq. (3.6) can also be derived using a Hamilton-Pontryagin variational principle (Bou-Rabee and Marsden, 2009). Given a discrete time-dependent trivialized Lagrangian $\bar{l}: \mathbb{Z} \times G \times \mathfrak{g} \rightarrow \mathbb{R}$, define the discrete Lagrangian in Hamilton-Pontryagin form

$$\tilde{l}_k(z_k, z_{k+1}) := \bar{l}_k(g_k, \xi_k) + \langle p_k, \tau^{-1}(\Delta g_k) - \xi_k \rangle,$$

where $z_k = (g_k, \xi_k, p_k) \in G \times \mathfrak{g} \times \mathfrak{g}^*$. The DEL equations (F.3) for such a Lagrangian read

$$\left\langle D_1 \tilde{l}_k(z_k, z_{k+1}) + D_2 \tilde{l}_{k-1}(z_{k-1}, z_k), \delta z_k \right\rangle = 0$$

for any variation δz_k . This equation decomposes with respect to $\delta z_k = (\delta g_k, \delta \xi_k, \delta p_k)$ into

$$\delta g: p_k \circ \mathbb{T}_{\Delta g_k} \tau^{-1} \circ \mathbb{L}_{g_k^{-1}} + \partial_g \bar{l}_{k+1}(g_{k+1}, \xi_{k+1}) - p_{k+1} \circ \mathbb{T}_{\Delta g_{k+1}} \tau^{-1} \circ \mathbb{L}_{g_{k+1}^{-1}} \circ \mathbb{R}_{\Delta g_{k+1}} = 0,$$

$$\delta \xi: \partial_\xi \bar{l}_k(g_k, \xi_k) - p_k = 0,$$

$$\delta p: \tau^{-1}(\Delta g_k) - \xi_k = 0,$$

which, after pulling the first to the identity, time-shifting the second, and using the definitions of Appendix A, is rewritten in the form

$$g_{k+1} = g_k \tau(\xi_k), \quad (3.9a)$$

$$p_{k+1} = \partial_\xi \bar{l}_{k+1}(g_{k+1}, \xi_{k+1}), \quad (3.9b)$$

$$(\mathrm{d}\tau_{\xi_{k+1}}^{-1})^* p_{k+1} = \mathrm{Ad}_{\Delta g_k}^* (\mathrm{d}\tau_{\xi_k}^{-1})^* p_k + \mathbb{L}_{g_{k+1}}^* \partial_g \bar{l}_{k+1}(g_{k+1}, \xi_{k+1}). \quad (3.9c)$$

Had we defined the discrete Lagrangian in this alternate form

$$\tilde{l}_k(z_k, z_{k+1}) := \bar{l}_k(g_k, \xi_k) + \langle p_{k+1}, \tau^{-1}(\Delta g_k) - \xi_{k+1} \rangle,$$

we would have ended up with the variational integrator

$$g_{k+1} = g_k \tau(\xi_{k+1}), \quad (3.10a)$$

$$p_{k+1} = \partial_\xi \bar{l}_{k+1}(g_{k+1}, \xi_{k+1}), \quad (3.10b)$$

$$(\mathrm{d}\tau_{\xi_{k+1}}^{-1})^* p_{k+1} = \mathrm{Ad}_{\Delta g_k}^* (\mathrm{d}\tau_{\xi_k}^{-1})^* p_k + \mathbb{L}_{g_k}^* \partial_g \bar{l}_k(g_k, \xi_k). \quad (3.10c)$$

Assume the Lagrangian is left-invariant, that is, assume $\partial_g \bar{l}_k = 0 \in \mathfrak{g}^*$, and redefine the momenta as $P_k := (\mathrm{d}\tau_{\xi_k}^{-1})^* p_k$, then the scheme (3.9) can be rewritten as follows

$$g_{k+1} = g_k \tau(\xi_{k+1}),$$

$$P_{k+1} = \mathrm{Ad}_{\Delta g_k}^* P_k,$$

$$P_{k+1} = (\mathrm{d}\tau_{\xi_{k+1}}^{-1})^* \partial_\xi \bar{l}_{k+1}(g_{k+1}, \xi_{k+1}),$$

which is explicit except for the last equation. Similarly, the scheme (3.10) is backward (in time) explicit. In fact, Equations (3.9) and (3.10) correspond, respectively, to Euler forward and backward methods (compare with Bou-Rabee and Marsden, 2009, Eqs. (4.19) and (4.20), which are similar but slightly different).

For the particular case of the Lagrangian (3.4a) or, rather, for the trivialized Lagrangian

$$\bar{l}_k(g, \xi) := l_k(g, g\tau(\xi)) = a_k \frac{1}{2} \|\xi\|^2 - b_k^- \phi(g) - b_{k+1}^+ \phi(g\tau(\xi)),$$

equation (3.9c) is equivalent to Equation (3.5a) (with $\varepsilon = 0$). To see this, simply compute the differential maps

$$\begin{aligned} \partial_g \bar{l}_k(g_0, \xi_0) &= -b_k^- \mathrm{d}\phi(g_0) - b_{k+1}^+ \mathrm{d}\phi(g_1) \circ \mathbb{R}_{\Delta g_0} \\ &= -b_k^- \mathbb{R}_{g_0^{-1}}^* \nabla \phi(g_0)^\flat - b_{k+1}^+ \mathbb{R}_{g_0^{-1}}^* \nabla \phi(g_1)^\flat, \\ \partial_\xi \bar{l}_k(g_0, \xi_0) &= a_k \xi_0^\flat - b_{k+1}^+ \mathrm{d}\phi(g_1) \circ \mathbb{L}_{g_0} \circ \mathbb{T}_{\xi_0} \tau \\ &= a_k \xi_0^\flat - b_{k+1}^+ (\mathrm{d}\tau_{\xi_0})^* \mathrm{Ad}_{g_0}^* \nabla \phi(g_1)^\flat, \end{aligned}$$

written in terms of the gradient and the trivialized tangent, and take into account the “definitions” (3.9b) and (3.5b).

4. Examples

4.1 Solvers for the reconstruction equation (3.6d)

The benchmark examples to be considered are defined on the groups of spatial rotations, $SO(3)$. Natural or common retraction maps on $\mathfrak{so}(3)$ are the matrix exponential (Appendix D) and the Cayley transform (Appendix C). Another case of interest is the skewsymmetric part of a rotation, the inverse of a certain retraction (Appendix E).

Before we define specific objective functions to be optimized, we must first observe that Equation (3.6d) can be rendered explicit for the selected retractions. In fact, in these cases, it is equivalent to the following expressions

$$R_{k+1} = R_k \exp(\Delta x_k), \quad R_{k+1} = \exp(\Delta x_k) R_k, \quad (4.1a)$$

$$R_{k+1} = R_k \operatorname{cay}(2\lambda \Delta x_k), \quad R_{k+1} = \operatorname{cay}(2\lambda \Delta x_k) R_k, \quad (4.1b)$$

$$R_{k+1} = R_k \operatorname{unskew}(\gamma \Delta x_k), \quad R_{k+1} = \operatorname{unskew}(\gamma \Delta x_k) R_k, \quad (4.1c)$$

where left and right equations correspond to the choice of left or right acting group transitions, respectively, and where for the Cayley transform the coefficient λ is given by

$$\lambda = \frac{1}{1 + (\Lambda - \frac{1}{3\Lambda})^2} \quad \text{with} \quad \Lambda = \sqrt[3]{\|\Delta x_k\| + \sqrt{\|\Delta x_k\|^2 + \frac{1}{27}}},$$

and where for the inverse skewsymmetric projection the coefficient is

$$\gamma = \frac{1}{1 + \sqrt{1 - \|\Delta x_k\|^2}}.$$

Indeed, Equation (3.5b) is equivalent to

$$\left(d\tau_{\tau^{-1}(\Delta g_k)}^{-1} \right)^t (\tau^{-1}(\Delta g_k)) = \operatorname{Ad}_{g_k}^t (\Delta x_k).$$

For $\tau = \exp: SO(3) \rightarrow \mathfrak{so}(3)$, this relation reads

$$\operatorname{dlog}(\log(\Delta R_k))^t (\log(\Delta R_k)) = \operatorname{Ad}_{R_k}^t (\Delta x_k).$$

Since $\operatorname{dlog}(\hat{x})^t(x) = x$ (confer with Equations (D.2a) and (D.2d)), we get

$$\log(\Delta R_k) = R_k^t \Delta x_k R_k,$$

which finally gives Equation (4.1a) (right, left is analogous),

$$R_{k+1} = R_k \exp(R_k^t \Delta x_k R_k) = \exp(\Delta x_k) R_k$$

where we have used the fact that the exponential map commutes with conjugation.

The case for the Cayley transform is slightly different, since $\operatorname{dcay}^{-1}(\hat{x})^t(x) = \frac{1+\|x\|^2}{2}x$ (confer with Equations (C.2a) and (C.2d)). Still, an identical derivation yields

$$\frac{1+\|\Omega_k\|^2}{2}\Omega_k = \operatorname{dcay}^{-1}(\hat{\Omega}_k)^t(\Omega_k) = R_k^t \Delta x_k R_k,$$

where $\hat{\Omega}_k = \text{cay}^{-1}(\Delta R_k)$. Applying the norm to both sides results in

$$\|\Omega_k\|^3 + \|\Omega_k\| - 2\|\Delta x_k\| = 0,$$

a third order algebraic equation for $\|\Omega_k\|$ with a single real root, $\Lambda - \frac{1}{3\Lambda}$, as in Equation (4.1b), which is proven once the commutation between the Cayley transform and the conjugation is taken into account,

$$R_{k+1} = R_k \text{cay} \left(\frac{2}{1+\|\Omega_k\|^2} R_k^t \Delta x_k R_k \right) = \text{cay} \left(\frac{2}{1+\|\Omega_k\|^2} \Delta x_k \right) R_k.$$

4.2 Objective functions

We consider four different functions defined by restriction or retraction.

4.2.1 RESTRICTED SQUARED FROBENIUS NORM

Consider the Frobenius (or entrywise) norm on the space of squared matrices $\mathcal{M}_{3 \times 3}(\mathbb{R})$ and let $f: \mathcal{M}_{3 \times 3}(\mathbb{R}) \rightarrow \mathbb{R}$, $A \mapsto \frac{1}{2}\|A - I\|^2$. We define

$$\phi := f|_{SO(3)}, \text{ for which } \nabla \phi(R) = R^-. \quad (4.2)$$

Since f is continuous and $SO(3) \subset \mathcal{M}_{3 \times 3}(\mathbb{R})$ is compact, we know that ϕ attains its global minimum and maximum values (0 and 4), which in fact occurs respectively at the identity I and at rotations with -1 trace.

4.2.2 RESTRICTED ROSENBRACK FUNCTION

The Rosenbrock function (Rosenbrock, 1960/61), whose expression is

$$\text{ros}(x, y; a, b) = (a - x)^2 + b(y - x^2)^2,$$

with parameters $a, b > 0$, represents a banana-shaped flat-valley surrounded by steep walls with a unique critical point and global minimum at a, a^2 , whose search by numerical means is difficult, hence its use to test and benchmark optimizers. We consider here its generalization to higher dimensions, $n > 2$, namely

$$\text{ros}(x) = \sum_{i=1}^{n-1} \text{ros}(x_i, x_{i+1}; 1, 100) = \sum_{i=1}^{n-1} [(1 - x_i)^2 + 100(x_{i+1} - x_i^2)^2]. \quad (4.3)$$

As in the two-dimensional case, the function has a global minimum at $(1, 1, \dots, 1)$ but, unlike it, also has a local minimum close to $(-1, 1, \dots, 1)$ (the higher is the dimension, the closer it gets).

Consider the function $g: \mathcal{M}_{3 \times 3}(\mathbb{R}) \rightarrow \mathbb{R}$, $A \mapsto \text{ros}(\mathbf{1} + A - I)$, where $\mathbf{1}$ is a matrix filled with 1's, and where the entries of the matrix to apply the Rosenbrock function ought to be taken columnwise. We define by restriction

$$\phi := g|_{SO(3)}, \text{ for which } \nabla \phi(R) = (\nabla \text{ros}(\mathbf{1} + R - I) \cdot R^t)^-. \quad (4.4)$$

The unique global minimum is attained at the identity I and is surrounded by other local minima. The global maximum is presumably at $\frac{1}{3}(2\mathbf{1} - 3I)$.

4.2.3 RETRACTED ROSENBROCK FUNCTION

As objective function, we consider a composition of either of the chosen retractions with the Rosenbrock function in \mathbb{R}^3 , that is,

$$\phi(R) := \text{ros}(\tau^{-1}(R)^\vee), \quad \forall R \in SO(3), \quad (4.5a)$$

where $\text{ros}(x, y, z) = (1 - x)^2 + 100 \cdot (y - x^2)^2 + (1 - y)^2 + 100 \cdot (z - y^2)^2$. It is then readily seen that the objective function ϕ has a unique global minimum at $\tau(\widehat{(1, 1, 1)})$.

To compute $\nabla\phi$, given $R \in SO(3)$, let $\hat{\Omega} = \tau^{-1}(R) \in \mathfrak{so}(3)$, and take $\hat{\Theta} \in \mathfrak{so}(3)$ arbitrary, then we get

$$\begin{aligned} \langle \nabla\phi(R), \hat{\Theta} \rangle &= d\phi(R)(\hat{\Theta}R) \\ &= \text{dros}(\Omega) \cdot (\mathbb{T}_{\tau(\hat{\Omega})}\tau^{-1}(\hat{\Theta}R))^\vee \\ &= \text{dros}(\Omega) \cdot ((\mathbb{T}_{\hat{\Omega}}\tau)^{-1}(\hat{\Theta}R))^\vee \\ &= \text{dros}(\Omega) \cdot d\tau^{-1}(\hat{\Omega})(\Theta) \\ &= \langle \nabla\text{ros}(\Omega), d\tau^{-1}(\hat{\Omega})(\Theta) \rangle \\ &= \langle (d\tau^{-1}(\hat{\Omega}))^t \cdot \nabla\text{ros}(\Omega), \Theta \rangle. \end{aligned}$$

where we have applied (in order) the trivialized gradient definition, the chain rule, the inverse function theorem, the trivialized tangent definition, the regular gradient definition, and the linear map transposition. Therefore, for the particular cases of the exponential and the Cayley transform (see (D.2d) and (C.2d)), we have

$$\nabla\phi(R) = (d\tau^{-1}(-\hat{\Omega}) \cdot \nabla\text{ros}(\Omega))^\wedge. \quad (4.5b)$$

5. Experiments and results

Several experiments have been conducted, and we present but a meaningful subset in the following figures. The plots illustrate the distance error on a logarithmic scale relative to the argument minimum of the objective functions described in the preceding Section 4.2. We consider three optimization methods: gradient descent (orange), Polyak's heavy ball (blue), and Nesterov's accelerated gradient (green). Additionally, a straight reference line (red) represents the slope for NAG. Our exploration involves two solvers: one (left) is based on the exponential map, Eq. (4.1a); the other (right) employs the Cayley transform, Eq. (4.1b). We ruled out the reconstruction equation solver based on the skew-symmetric matrix projection, as it gives similar results to the one base on the exponential map. The chosen strategies (aggressive, $\mu_0 = 0.7$, $\eta_0 = 0.1$; mild, $\mu_0 = 0.9$, $\eta_0 = 0.01$; conservative, $\mu_0 = 0.99$, $\eta_0 = 0.0001$) are constant and they are derived (approximately) from an exponentially dilated Lagrangian (cf. with Campos et al., 2023).

The experiments were implemented in Julia v1.8 and are available at an open access repository, <https://github.com/cmcampos-xyz>. They only pretend to show that, in general, the schemes perform as expected, but do not for particular cases that we highlight.

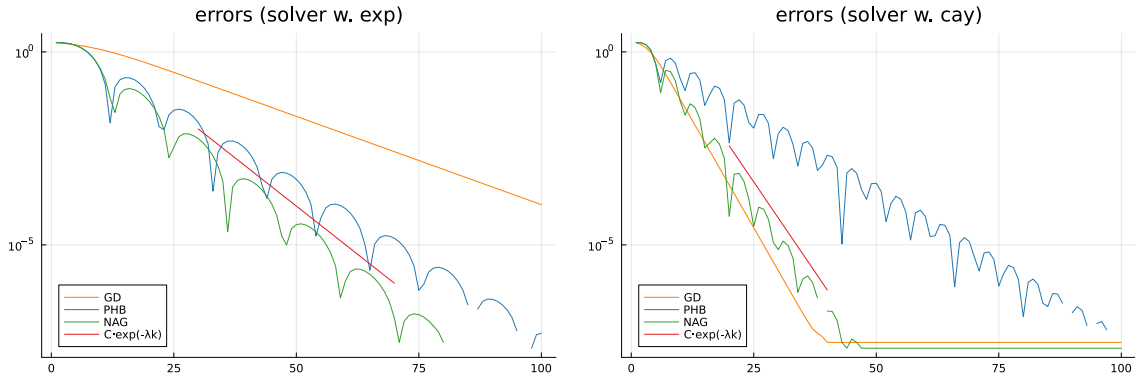


Figure 1: Error *vs.* epoch plot in log scale for the restricted Frobenius norm. Simulation run for 100 epochs from initial guess $R_0 = \text{cay}(1, 1, 1)$ with constant strategy $\mu_0 = 0.7$ (0 for GD), $\eta_0 = 0.1$.

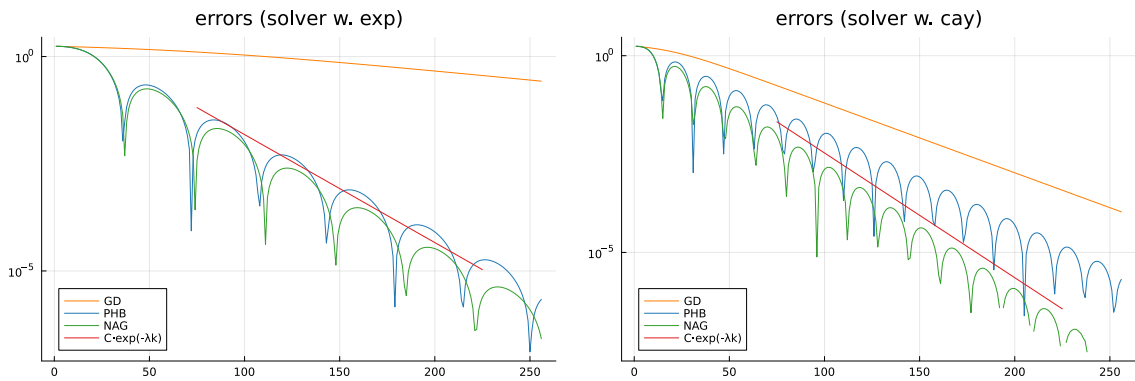


Figure 2: Error *vs.* epoch plot in log scale for the restricted Frobenius norm. Simulation run for 250 epochs from initial guess $R_0 = \text{cay}(1, 1, 1)$ with constant strategy $\mu_0 = 0.9$ (0 for GD), $\eta_0 = 0.01$.

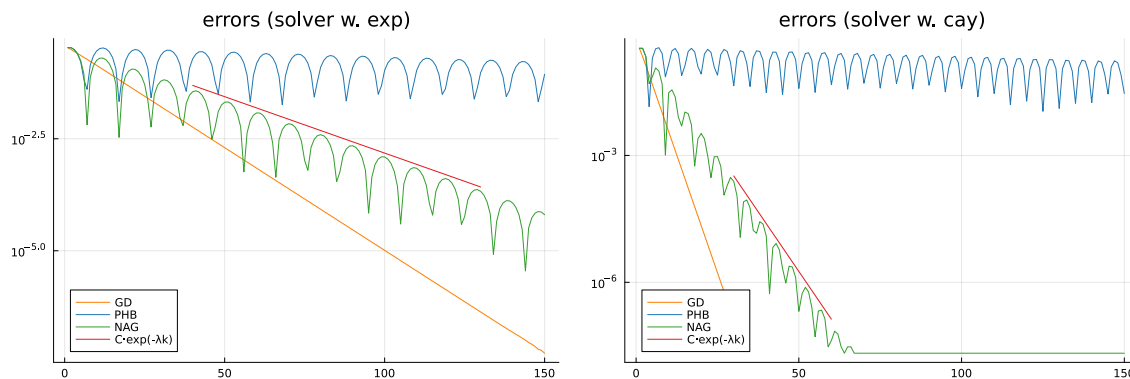


Figure 3: Error *vs.* epoch plot in log scale for the restricted Rosenbrock function. Simulation run for 150 epochs from initial guess $R_0 = \text{cay}(0.1, 0.1, 0.1)$ with constant strategy $\mu_0 = 0.99$ (0 for GD), $\eta_0 = 0.0001$.

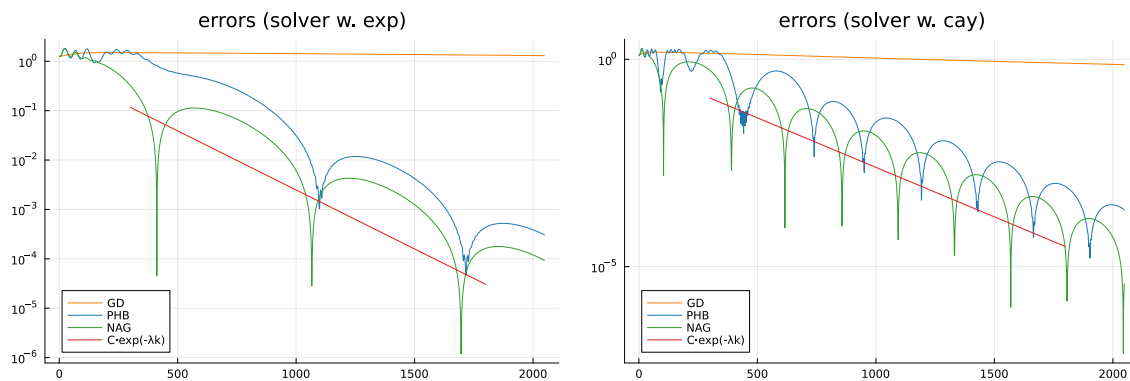


Figure 4: Error *vs.* epoch plot in log scale for the Rosenbrock function retracted by $\tau = \text{exp}$. Simulation run for 2000 epochs from initial guess $R_0 = \text{exp}(0, 0, 1)$ with constant strategy $\mu_0 = 0.99$ (0 for GD), $\eta_0 = 0.0001$.

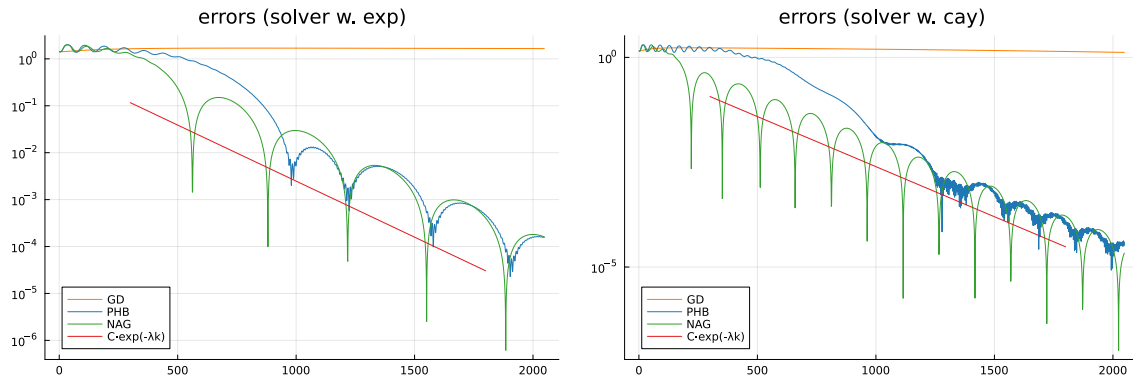


Figure 5: Error *vs.* epoch plot in log scale for the Rosenbrock function retracted by $\tau = \text{cay}$. Simulation run for 2000 epochs from initial guess $R_0 = \text{cay}(0, 0, 1)$ with constant strategy $\mu_0 = 0.99$ (0 for GD), $\eta_0 = 0.0001$.

This shows that a numerical analysis, out of the scope of the present paper, is nonetheless of interest.

We observe that in most cases, as expected, NAG outperforms PHB and both outperform GD, but this not always the case depending on the chosen solver or strategy. For instance, in Fig. 1 (right), when optimizing the squared Frobenius norm for a “small” momentum coefficient coupled with a “big” learning rate (that is, a big time step) while using the Cayley transform, GD outperforms clearly PHB and slightly NAG. However, this is no longer the case when a less aggressive strategy is considered, Fig. 2, giving the expected result. Both figures correspond the simplest objective function, the squared Frobenius norm.

In the case of the 9-dimensional Rosenbrock function, Fig. 3, even with the considered conservative strategy, PHB is surpassed by GD, and NAG surpasses GD only in the Cayley case. More conservative strategies would give results similar to those in Figs. 1 and 2. On the contrary, a more aggressive strategy would move away from the argument minimum, even with a much closer initial guess.

For both versions of the retracted Rosenbrock function, Figs. 4 and 5, we observe the expected result, a clear improvement by using momentum methods over GD.

6. Conclusions

We present a variational derivation of first-order momentum methods for Lie groups. These schemes generalize the well-known PHB and NAG methods in \mathbb{R}^n . These familiar methods emerge as special cases when considering the group of translations in \mathbb{R}^n with the identity as the retraction map. In fact, the methods applied to both Euclidean space and Lie groups share a common formal structure, albeit with few distinctions. As in general, a Lie group is not a linear space, we cannot write the right translation element $\Delta g_0 = g_0^{-1}g_1$ as the difference $g_1 - g_0$. To address this, we resort to pull the problem to the Lie algebra associated with the group. The intricate relationship between the group and its algebra is captured by a novel equation, termed the reconstruction equation. Apart from this equation, the

schemes are explicit, and in specific scenarios, this equation can also be rendered explicit. Notably, this holds true for the exponential map, the Cayley transform, and the inverse of the skew-symmetric projection. Furthermore, our method can be implemented either in terms of Δx_k using an overlapped approach or directly in terms of x_k by setting $x_0 = 0$.

The methods have been formulated by exploiting the inherent geometrical structure of these spaces. They are equivalent to the Euler-Lagrange equations of concrete Lagrangian systems. In addition, these methods can be expressed in Hamilton-Pontryagin form, which relate to the Euler forward and backward methods.

In general, numerical results align with expectations. However, there exist cases that deviate from this generality, highlighting the need for a more detailed numerical analysis. Such an analysis should consider not only the properties of the objective function, scheme, and strategy but also the geometric aspects of the Lie group, as conveyed through the retraction map.

Acknowledgements

CMC and DMdD acknowledge financial support from the Spanish Ministry of Science and Innovation, under grants PID2022-137909NB-C21, TED2021-129455B-I00 and CEX2019-000904-S funded by MCIN/AEI/10.13039/501100011033. DMdD acknowledges financial support from BBVA Foundation via the project ‘‘Mathematical optimization for a more efficient, safer and decarbonized maritime transport’’.

A. Retractions on Lie groups

Let G be a Lie group, TG denotes the tangent bundle, $\mathfrak{g} = T_e G$ its Lie algebra, where e is the neutral element of G , and T^*G and \mathfrak{g}^* their duals. The left and right actions (or translations) of the group are denoted L_g and R_h , respectively, so that $L_g(h) = gh = R_h(g)$. It readily seen that left and right translation commute, that is, $L_g \circ R_h = R_h \circ L_g$. Moreover, these maps allow for the trivialization of the tangent and cotangent bundles. For the left action:

$$\begin{aligned} TG &\longrightarrow G \times \mathfrak{g} & T^*G &\longrightarrow G \times \mathfrak{g}^* \\ (g, \dot{g}) &\longmapsto (g, T_g L_{g^{-1}} \dot{g}) & (g, \alpha) &\longmapsto (g, (T_e L_g)^* \alpha) \end{aligned}$$

Analogously for the right action.

The *conjugation* is the map $C_g := L_g \circ R_{g^{-1}}: G \rightarrow G$, the *adjoint group representation* is $\text{Ad}: G \rightarrow \text{Gl}(\mathfrak{g})$ such that $\text{Ad}_g := T_e C_g: \mathfrak{g} \rightarrow \mathfrak{g}$, and the *adjoint algebra representation* is $\text{ad} := T_e \text{Ad}: \mathfrak{g} \rightarrow \mathfrak{gl}(\mathfrak{g})$ so that $\text{ad}_\xi \eta = [\xi, \eta]$.

A *retraction* on G is a mapping $\tau: \mathfrak{g} \rightarrow G$, which is an analytic local diffeomorphism around the identity such that $\tau(\xi)\tau(-\xi) = e$ for any $\xi \in \mathfrak{g}$. Thereby, τ provides a local chart on the Lie group. A particular case of retraction is the exponential map.

Given a retraction $\tau: \mathfrak{g} \rightarrow G$, we define its *right-trivialized tangent* (Bou-Rabee and Marsden, 2009) as the mapping $d\tau: \mathfrak{g} \times \mathfrak{g} \rightarrow \mathfrak{g}$ given for any $\xi \in \mathfrak{g}$ by

$$d\tau(\xi, \cdot) = d\tau_\xi := T_g R_{g^{-1}} \circ T_\xi \tau, \tag{A.1}$$

where $g = \tau(\xi)$, therefore $g^{-1} = \tau(\xi)^{-1} = \tau(-\xi)$. The *right-trivialized inverse tangent* of τ is the mapping $d\tau^{-1}: \mathfrak{g} \times \mathfrak{g} \rightarrow \mathfrak{g}$

$$d\tau^{-1}(\xi, \cdot) = d\tau_{\xi}^{-1} := (d\tau_{\xi})^{-1} = T_g\tau^{-1} \circ T_e R_g . \quad (\text{A.2})$$

The left-trivialized direct and inverse tangent are defined analogously.

The trivialized tangents have a simple relation with the adjoint group representation:

$$d\tau_{\xi} = \text{Ad}_{\tau(\xi)} d\tau_{-\xi} , \quad d\tau_{\xi}^{-1} = d\tau_{-\xi}^{-1} \text{Ad}_{\tau(-\xi)} . \quad (\text{A.3})$$

A.1 The group of rotations in \mathbb{R}^3

The special orthogonal group of \mathbb{R}^3 , denoted $SO(3)$, is the set of rotations of \mathbb{R}^3 which can be identified with the group of orthogonal 3×3 matrices with positive determinant. Other possible identifications are with the real projective space $\mathbb{P}^3(\mathbb{R})$, or with the closed ball of radius π whose surface is “glued” together at antipodal points. A vector in such set identifies with the axis of the rotation and its length gives the rotation angle, being 0 the identity.

The Lie algebra associated to $SO(3)$ (and $O(3)$), denoted $\mathfrak{so}(3)$, consists (under identification) of the skew-symmetric 3×3 matrices. Besides of the exponential map, which (under identification) corresponds here to the matrix exponential (Appendix D), another example of retraction is the Cayley transform (Appendix C).

B. Matrix identities

We summarize here some identities that relate common operations in \mathbb{R}^3 : the scalar product, the tensor product, the cross product, and the hat map. We recall that

$$x = (x_1, x_2, x_3) \in \mathbb{R}^3 \mapsto \hat{x} = \begin{pmatrix} 0 & -x_3 & x_2 \\ x_3 & 0 & -x_1 \\ -x_2 & x_1 & 0 \end{pmatrix} \in \mathfrak{so}(3), \quad \text{with inverse } (\hat{x})^\vee = x .$$

$$(x \otimes x)(y) = \langle x, y \rangle x \quad (\text{B.1a})$$

$$x \otimes x = \|x\|^2 I + \hat{x}^2 \quad (\text{B.1b})$$

$$\hat{x}y = x \times y \quad (\text{B.1c})$$

$$\hat{x}\hat{y} = y \otimes x - \langle x, y \rangle I \quad (\text{B.1d})$$

$$\hat{x}\hat{y} - \hat{y}\hat{x} = \widehat{x \times y} \quad (\text{B.1e})$$

$$\hat{x}\hat{y}\hat{x} = -\langle x, y \rangle \hat{x} \quad (\text{B.1f})$$

$$\hat{x}^2\hat{y} + \hat{y}\hat{x}^2 = -\|x\|^2\hat{y} - \langle x, y \rangle \hat{x} \quad (\text{B.1g})$$

$$\hat{x}^3 = -\|x\|^2\hat{x} \quad (\text{B.1h})$$

$$\text{tr}(\hat{x}^2) = -2\|x\|^2 \quad (\text{B.1i})$$

$$\left(\frac{\text{tr}(R)-1}{2}\right)^2 + \|(R^-)^\vee\|^2 = 1 \quad (\text{B.1j})$$

C. The Cayley transform

The Cayley transform is the map

$$\text{cay}: \hat{x} \in \mathfrak{so}(3) \longmapsto (I - \hat{x})^{-1}(I + \hat{x}) \in SO(3). \quad (\text{C.1})$$

Indeed, $\text{cay}(\hat{x})^t \text{cay}(\hat{x}) = I$. We then have the formulas

$$\text{cay}(\hat{x}) = I + 2\lambda\hat{x} + 2\lambda\hat{x}^2, \quad (\text{C.2a})$$

$$\text{cay}^{-1}(R) = \frac{2}{1+\text{tr}(R)}R^-, \quad (\text{C.2b})$$

$$\text{dcay}(\hat{x}) = 2\lambda(I \pm \hat{x}), \quad (\text{C.2c})$$

$$\text{dcay}^{-1}(\hat{x}) = \frac{1}{2}(I \mp \hat{x} + x \otimes x), \quad (\text{C.2d})$$

where $\lambda := \frac{1}{1+\|x\|^2}$, $\text{dcay}(\hat{x})(y) := ((A_{\text{cay}(\hat{x})^{-1}} \circ T_{\hat{x}} \text{cay})(\hat{y}))^\vee$, and $\text{dcay}^{-1}(\hat{x}) := (\text{dcay}(\hat{x}))^{-1}$. The lower\upper signs in (C.2c) and (C.2d) correspond to the choice $A = L \setminus R$, the left\right action, respectively.

$$\begin{array}{ccc} \mathfrak{so}(3) \cong T_{\hat{x}}\mathfrak{so}(3) & \xrightarrow{T_{\hat{x}} \text{cay}} & T_{\text{cay}(\hat{x})}SO(3) \xrightarrow{A_{\text{cay}(\hat{x})^{-1}}} T_I SO(3) \cong \mathfrak{so}(3) \\ \uparrow \wedge & & \downarrow \vee \\ \mathbb{R}^3 & \xleftarrow{\text{dcay}(\hat{x})} & \mathbb{R}^3 \xrightarrow{\text{dcay}^{-1}(\hat{x})} \end{array}$$

We first show that

$$(I - \hat{x})^{-1} = I + \lambda\hat{x} + \lambda\hat{x}^2. \quad (\text{C.3})$$

Indeed, carry out the following product and use (B.1h) to get

$$(I + \lambda\hat{x} + \lambda\hat{x}^2)(I - \hat{x}) = I + \lambda\hat{x} + \lambda\hat{x}^2 - \hat{x} - \lambda\hat{x}^2 - \lambda\hat{x}^3 = I + (\lambda - 1 + \lambda\|x\|^2)\hat{x} = I.$$

An almost identical development using now (C.3) in definition (C.1) gives formula (C.2a),

$$(I + \lambda\hat{x} + \lambda\hat{x}^2)(I + \hat{x}) = I + \lambda\hat{x} + \lambda\hat{x}^2 + \hat{x} + \lambda\hat{x}^2 + \lambda\hat{x}^3 = I + (\lambda + 1 - \lambda\|x\|^2)\hat{x} + 2\lambda\hat{x}^2.$$

Besides, (C.3) also gives the commutativity of the factors in (C.1),

$$(I - \hat{x})^{-1}(I + \hat{x}) = (I + \hat{x})(I - \hat{x})^{-1}.$$

For the inverse transform, cay^{-1} , define $R := \text{cay}(\hat{x})$ to obtain thanks to Equations (C.2a) and (B.1i)

$$\text{tr}(R) = \text{tr}(I) + 2\lambda \text{tr}(\hat{x}^2) = 3 - 4\lambda\|x\|^2 = 4\lambda - 1,$$

or, equivalently,

$$2\lambda = \frac{1}{2}(1 + \text{tr}(R)).$$

Since $R^- = 2\lambda\hat{x}$, we deduce formula (C.2b). Moreover, from this same formula and the definition of λ , we get the relation

$$1 + \|x\|^2 =: \lambda^{-1} = 2 \cdot \frac{2}{1+\text{tr}(R)}.$$

Taking into account that now we have $\|x\| = \frac{2}{1+\text{tr}(R)}\|(R^-)^\vee\|$ from (C.2b), we get

$$1 + \left(\frac{2}{1+\text{tr}(R)}\right)^2\|(R^-)^\vee\|^2 = 2 \cdot \frac{2}{1+\text{tr}(R)}.$$

Multiply by $\left(\frac{1+\text{tr}(R)}{2}\right)^2$, pull everything to the left hand side,

$$\left(\frac{1+\text{tr}(R)}{2}\right)^2 - 2 \cdot \frac{1+\text{tr}(R)}{2} + \|(R^-)^\vee\|^2 = 0,$$

and complete squares to obtain the trigonometric relation (B.1j) between the trace of a rotation and the norm of its skewsymmetric part.

For the tangent map, simple derivation yields

$$\begin{aligned} (\mathbb{T}_{\hat{x}} \text{cay})(\hat{y}) &:= \frac{d}{dt} [\text{cay}(\hat{x}(t))] |_{t=0} : \hat{x}(0) = \hat{x} \ \& \ \frac{d}{dt} \hat{x}(t) |_{t=0} = \hat{y} \\ &= (I - \hat{x})^{-1} \hat{y} (I - \hat{x})^{-1} (I + \hat{x}) + (I - \hat{x})^{-1} \hat{y} \\ &= (I - \hat{x})^{-1} \hat{y} (\text{cay}(\hat{x}) + I) \\ &= 2(I - \hat{x})^{-1} \hat{y} (I - \hat{x})^{-1}. \end{aligned}$$

Pulling to the identity by the left action (right action is analogous) results in

$$\begin{aligned} \widehat{\text{dcay}(\hat{x})}(y) &:= \text{cay}(\hat{x})^{-1} \cdot (\mathbb{T}_{\hat{x}} \text{cay})(\hat{y}) \\ &= \text{cay}(-\hat{x}) \cdot (\mathbb{T}_{\hat{x}} \text{cay})(\hat{y}) \\ &= 2(I + \hat{x})^{-1} \hat{y} (I - \hat{x})^{-1}. \end{aligned}$$

Instead of developing this expression, we work around it by computing first its inverse,

$$\begin{aligned} \widehat{\text{dcay}^{-1}(\hat{x})}(y) &:= \widehat{\text{dcay}(\hat{x})^{-1}}(y) \\ &= \frac{1}{2}(I + \hat{x}) \hat{y} (I - \hat{x}) \\ &= \frac{1}{2}(\hat{y} + \hat{x} \hat{y} - \hat{y} \hat{x} - \hat{x} \hat{y} \hat{x}) \\ &= \frac{1}{2}(\hat{y} + \widehat{x \times y} + \langle x, y \rangle \hat{x}). \end{aligned}$$

Equations (B.1c) and (B.1a) show the desired result, (C.2d), which in turn is used in conjunction with (B.1b) and (C.3) to show (C.2c),

$$\begin{aligned} \text{dcay}^{-1}(\hat{x}) &= \frac{1}{2}(I + \hat{x} + x \otimes x) \\ &= \frac{1}{2}((1 + \|x\|^2)I + \hat{x} + \hat{x}^2) \\ &= \frac{1}{2\lambda}(I - \hat{x})^{-1}. \end{aligned}$$

D. The matrix exponential in $\mathfrak{so}(3)$

The matrix exponential is the map

$$\exp: A \in \mathfrak{gl}(n) \longmapsto \sum_{k=0}^{\infty} \frac{A^k}{k!} \in GL(n), \quad (\text{D.1})$$

whose restriction to $\mathfrak{so}(3)$ gives a map $\exp: \mathfrak{so}(3) \rightarrow SO(3)$. We then have the formulas

$$\exp(\hat{x}) = I + \frac{\sin \omega}{\omega} \hat{x} + \frac{1 - \cos \omega}{\omega^2} \hat{x}^2 \quad (\text{D.2a})$$

$$\log(R) = \frac{\cos^{-1} \left(\frac{\text{tr}(R) - 1}{2} \right)}{\|(R^-)^\vee\|} R^- \quad (\text{D.2b})$$

$$\text{dexp}(\hat{x}) = I \pm \frac{1}{2} \frac{\sin(\omega/2)}{(\omega/2)^2} \hat{x} + \frac{\omega - \sin(\omega)}{\omega^3} \hat{x}^2 \quad (\text{D.2c})$$

$$\text{dlog}(\hat{x}) = I \mp \frac{1}{2} \hat{x} + \frac{1}{2} \frac{2 - \omega \cot(\omega/2)}{\omega^2} \hat{x}^2 \quad (\text{D.2d})$$

where $\omega = \|\hat{x}\|$. As in (C.2), the lower\upper signs in (D.2c) and (D.2d) correspond to the choice $A = L \setminus R$, the left\right action, respectively.

$$\begin{array}{ccc} \mathfrak{so}(3) \cong T_{\hat{x}} \mathfrak{so}(3) & \xrightarrow{T_{\hat{x}} \exp} & T_{\exp(\hat{x})} SO(3) \xrightarrow{A_{\exp(\hat{x})}^{-1}} T_I SO(3) \cong \mathfrak{so}(3) \\ \uparrow \wedge & & \downarrow \vee \\ \mathbb{R}^3 & \xleftrightarrow{\text{dexp}(\hat{x})} & \mathbb{R}^3 \\ & \xleftarrow{\text{dlog}(\hat{x})} & \end{array}$$

Formula (D.2a) is easily obtained by splitting the exponential series in odd and even terms so that the sine and cosine series are recovered.

$$\begin{aligned} \exp(\hat{x}) &= \sum_{k=0}^{\infty} \frac{\hat{x}^k}{k!} \\ &= I + \sum_{k=0}^{\infty} \frac{\hat{x}^{2k+1}}{(2k+1)!} + \sum_{k=0}^{\infty} \frac{\hat{x}^{2k+2}}{(2k+2)!} \\ &= I + \sum_{k=0}^{\infty} (-1)^k \frac{\omega^{2k}}{(2k+1)!} \hat{x} + \sum_{k=0}^{\infty} (-1)^k \frac{\omega^{2k}}{(2k+2)!} \hat{x}^2 \\ &= I + \frac{1}{\omega} \left(\sum_{k=0}^{\infty} (-1)^k \frac{\omega^{2k+1}}{(2k+1)!} \right) \hat{x} - \frac{1}{\omega^2} \left(\sum_{k=0}^{\infty} (-1)^{k+1} \frac{\omega^{2k+2}}{(2k+2)!} \right) \hat{x}^2 \end{aligned}$$

For the logarithm, define $R := \exp(\hat{x})$. Formula (D.2a) readily gives $R^- = \frac{\sin \omega}{\omega} \hat{x}$, from which

$$\log(R) = \hat{x} = \frac{\omega}{\sin \omega} R^- \quad \text{and} \quad |\sin \omega| = \|(R^-)^\vee\|.$$

Also from (D.2a), and using (B.1i), we get $\text{tr}(R) = \text{tr}(I) + \frac{1 - \cos \omega}{\omega^2} \text{tr}(\hat{x}^2) = 1 + 2 \cos \omega$ or, equivalently,

$$\cos \omega = \frac{\text{tr}(R) - 1}{2},$$

which show (D.2b) for $\omega \in [0, \pi]$. Besides, the trigonometric relations give (B.1j) too.

For the time being, let

$$a(\omega) := \frac{\sin \omega}{\omega}, \quad b(\omega) := \frac{1 - \cos \omega}{\omega^2}, \quad \text{and} \quad \gamma := \langle x, y \rangle / \omega,$$

so that simple derivation yields for the tangent map

$$\begin{aligned} (T_{\hat{x}} \exp)(\hat{y}) &:= \frac{d}{dt} [\exp(\hat{x}(t))] |_{t=0} : \hat{x}(0) = \hat{x} \ \& \ \frac{d}{dt} \hat{x}(t) |_{t=0} = \hat{y} \\ &= a' \cdot \gamma \cdot \hat{x} + a \cdot \hat{y} + b' \cdot \gamma \cdot \hat{x} + b \cdot (\hat{x} \hat{y} + \hat{y} \hat{x}). \end{aligned}$$

Pulling to the identity by the left action (right action is analogous) results in

$$\begin{aligned}
 \widehat{\text{dexp}}(\hat{x})(y) &:= \exp(\hat{x})^{-1} \cdot (\mathbb{T}_{\hat{x}} \exp)(\hat{y}) \\
 &= \exp(-\hat{x}) \cdot (\mathbb{T}_{\hat{x}} \exp)(\hat{y}) \\
 &= a' \gamma \hat{x} + a \hat{y} + b' \gamma \hat{x}^2 + b \hat{x} \hat{y} + b \hat{y} \hat{x} \\
 &\quad - a a' \gamma \hat{x}^2 - a^2 \hat{x} \hat{y} - a b' \gamma \hat{x}^3 - a b \hat{x}^2 \hat{y} - a b \hat{x} \hat{y} \hat{x} \\
 &\quad + a' b \gamma \hat{x}^3 + a b \hat{x}^2 \hat{y} + b b' \gamma \hat{x}^4 + b^2 \hat{x}^3 \hat{y} + b^2 \hat{x}^2 \hat{y} \hat{x} \\
 &= (a' + a b' \omega^2 + a b \omega - a' b \omega^2) \gamma \hat{x} + a \hat{y} - \frac{1}{2} (a^2 + b^2 \omega^2) (\hat{x} \hat{y} - \hat{y} \hat{x}) \\
 &= (a' / \omega + a b' \omega + a b - a' b \omega) \langle x, y \rangle \hat{x} + a \hat{y} - \frac{1}{2} (a^2 + b^2 \omega^2) \widehat{x \times y}
 \end{aligned}$$

From formulas (B.1a) and (B.1c), we may write

$$\text{dexp}(\hat{x})(y) = aI - \frac{1}{2}(a^2 + b^2 \omega^2) \hat{x} + \left(\frac{a'}{\omega} + a b' \omega + a b - a' b \omega\right) x \otimes x$$

which is simplified using the expressions of a and b to get

$$\begin{aligned}
 &= aI - b\hat{x} + \frac{1-a}{\omega^2} x \otimes x \\
 &= I - b\hat{x} + \frac{1-a}{\omega^2} \hat{x}^2
 \end{aligned}$$

where (B.1b) has been used.

For its inverse (D.2d), we take a direct approach by developing

$$\left(I + \frac{1}{2}\hat{x} + \frac{1}{\omega^2}\left(1 - \frac{1}{2}\frac{a}{b}\right)\hat{x}^2\right) \text{dexp}(\hat{x}) = I + \frac{1}{\omega^2}\left(1 - \frac{1}{2}b\omega^2 - \frac{1}{2}\frac{a^2}{b}\right)\hat{x}^2 = I,$$

where the last term cancels proving the desired result.

E. The skewsymmetric matrix projection

The skewsymmetric matrix projection is the linear endomorphism

$$\text{skew}: A \in \mathcal{M}_{n \times n}(\mathbb{R}) \longmapsto A^- := \frac{1}{2}(A - A^t) \in \mathcal{M}_{n \times n}(\mathbb{R}). \quad (\text{E.1})$$

This map is indeed a projection that annihilates symmetric matrices and, therefore, it is not bijective. Its restriction to $SO(n)$ is however a local diffeomorphism around the identity whose inverse is the retraction map

$$\text{unskew}: A \in \mathfrak{so}(n) \longmapsto A + \sqrt{I + A^2} \in SO(n), \quad (\text{E.2})$$

where $\sqrt{I + A^2}$ is the unique positive definite matrix whose square is $I + A^2$ for A small enough (Cardoso and Leite, 2003; Th. 6.1). For the case $n = 3$, we have the following formulas

$$\text{unskew}(\hat{x}) = I + \hat{x} + \gamma \hat{x}^2 \quad (\text{E.3a})$$

$$\text{skew}(R) = \frac{1}{2}(R - R^t) \quad (\text{E.3b})$$

$$\text{dunskew}(\hat{x}) = \gamma I \pm \frac{\gamma}{3+2\gamma} \hat{x} + \frac{1+\gamma^2}{3+2\gamma} \hat{x}^2 \quad (\text{E.3c})$$

$$\text{dskew}(\hat{x}) = \gamma^{-1} I \mp \frac{1}{2} \hat{x} - \frac{1}{2} \gamma \hat{x}^2 \quad (\text{E.3d})$$

where $\gamma^{-1} = 1 + \sqrt{1 - \|x\|^2}$ (so here “small enough” means $0 \leq \|x\| < 1$). As in (C.2) and (D.2), the lower\upper signs in (E.3c) and (E.3d) correspond to the choice $A = L \setminus R$, the left\right action, respectively.

$$\begin{array}{ccc}
 \mathfrak{so}(3) \cong T_{\hat{x}}\mathfrak{so}(3) & \xleftarrow{T_R \text{skew}} & T_R SO(3) \xleftarrow{A_R} T_I SO(3) \cong \mathfrak{so}(3) \\
 \uparrow \wedge & & \downarrow \vee \\
 \mathbb{R}^3 & \xleftarrow{\text{dunskew}(\hat{x})} & \mathbb{R}^3 \\
 & \xrightarrow{\text{dskew}(\hat{x})} &
 \end{array}$$

Equation (E.3a) is easily proven if we observe that, for $x \in \mathbb{R}^3$ small enough, $\sqrt{I + \hat{x}^2} = I + \gamma \hat{x}^2$ since, by Eq. (B.1h), $(I + \gamma \hat{x}^2)^2 = I + \hat{x}^2$ and $I + \gamma \hat{x}^2$ is positive definite. Next we show Equation (E.3d). To this end, take $\hat{x} = \text{skew}(R)$ and compute

$$\begin{aligned}
 \widehat{\text{dskew}(\hat{x})}(y) &= T_R \text{skew}(\hat{y} \text{unskew}(\hat{x})) \\
 &= \text{skew}(\hat{y}(I + \hat{x} + \gamma \hat{x}^2)) \\
 &= \hat{y} + \frac{1}{2}(\hat{y}\hat{x} - \hat{x}\hat{y}) + \frac{1}{2}\gamma(\hat{y}\hat{x}^2 + \hat{x}^2\hat{y}) \\
 &= \hat{y} - \frac{1}{2}\widehat{x \times y} - \frac{1}{2}\gamma(\|x\|^2\hat{y} + \langle x, y \rangle \hat{x})
 \end{aligned}$$

which shows

$$\text{dskew}(\hat{x}) = I - \frac{1}{2}\hat{x} - \frac{1}{2}\gamma(\|x\|^2 I + x \otimes x).$$

In this, we have used the fact that $T_R \text{skew} = \text{skew}$ and the matrix identities (B.1), which in turn give (E.3d).

To show that (E.3d) is the inverse of (E.3c), simply expand the matrix product of both to get the identity.

F. Continuous and discrete Euler-Lagrange equations for Lie groups

In this section we recall the continuous and discrete Euler-Lagrange equations for systems with configuration a Lie group G (with Lie algebra \mathfrak{g}). In the continuous case the equations are determined prescribing a Lagrangian function $L: \mathbb{R} \times TG \rightarrow \mathbb{R}$ and, in the discrete case, by a discrete Lagrangian function $l: \mathbb{Z} \times G \times G \rightarrow \mathbb{R}$.

F.1 The continuous equations

Given a smooth manifold Q , let (q^i, \dot{q}^i) denote adapted coordinates on its tangent bundle TQ , a Lagrangian function $L: \mathbb{R} \times TQ \rightarrow \mathbb{R}$, and an external force $F: \mathbb{R} \times TQ \rightarrow T^*Q$ (a fibered map over Q). The Euler-Lagrange equations for the system (L, F) are

$$\frac{d}{dt} \left(\frac{\partial L}{\partial \dot{q}} \right) - \frac{\partial L}{\partial q} = F. \quad (\text{F.1})$$

These equations are still valid for a Lie group G , however they are usually rewritten in terms of left or right trivialization, $TG \cong G \times \mathfrak{g}$.

Given $L: \mathbb{R} \times TG \rightarrow \mathbb{R}$ and $F: \mathbb{R} \times TG \rightarrow T^*G$, define their right-trivializations $\bar{L}: \mathbb{R} \times G \times \mathfrak{g} \rightarrow \mathbb{R}$ and $\bar{F}: \mathbb{R} \times G \times \mathfrak{g} \rightarrow \mathfrak{g}^*$ by the expressions

$$\bar{L}(t, g, \xi) = L(t, g, R_g \xi), \quad \bar{F}(t, g, \xi) = R_g^*(F(t, g, R_g \xi)).$$

The right-trivialized Euler-Lagrange equation for (\bar{L}, \bar{F}) are

$$\frac{d}{dt} \left(\frac{\partial \bar{L}}{\partial \xi} \right) + \text{ad}_\xi^* \left(\frac{\partial \bar{L}}{\partial \xi} \right) - R_g^* \left(\frac{\partial \bar{L}}{\partial g} \right) = \bar{F}, \quad (\text{F.2})$$

which, together with the *reconstruction equation* $\dot{g} = \xi g$, are equivalent to Eq. (F.1).

Given smooth functions $a, b: \mathbb{R} \rightarrow \mathbb{R}_+$ and $\phi: G \rightarrow \mathbb{R}$, consider the right-trivialized Lagrangian

$$\bar{L}(t, g, \xi) = \frac{1}{2} a(t) \|\xi\|^2 - b(t) \phi(g),$$

where $\|\cdot\|$ is the norm associated to a given inner product $\langle \cdot, \cdot \rangle$ on the Lie algebra \mathfrak{g} . Then the right-trivialized Euler-Lagrange equation are

$$\frac{d}{dt} \left(a(t) \xi^b \right) + a(t) \text{ad}_\xi^* \xi^b - b(t) R_g^* d\phi(g) = 0 \in \mathfrak{g}^*,$$

that is, after expanding and using the sharp isomorphism,

$$\dot{\xi} + \text{ad}_\xi^t \xi + \frac{\dot{a}}{a} \xi - \frac{\dot{b}}{a} \nabla \phi(g) = 0 \in \mathfrak{g}.$$

F.2 The discrete equations

In this case, the phase space TQ is replaced by $Q \times Q$, while the continuous time line \mathbb{R} is replaced by discrete time ticks \mathbb{Z} . We therefore consider a time-dependent discrete Lagrangian $l: \mathbb{Z} \times Q \times Q \rightarrow \mathbb{R}$, otherwise a family $l_k: Q \times Q \rightarrow \mathbb{R}$, $k \in \mathbb{Z}$, and two families of external forces $f_k^\pm: Q \times Q \rightarrow T^*Q$ (fibered maps over Q along the projections pr_\pm). Then the discrete Euler-Lagrange equations for the system (l, f^\pm) are (confer with Campos et al., 2023, for this approach, and with Marsden and West, 2001, for an introduction to discrete Lagrangian mechanics):

$$D_1 l_k(q_k, q_{k+1}) + D_2 l_{k-1}(q_{k-1}, q_k) + f_k^-(q_k, q_{k+1}) + f_{k-1}^+(q_{k-1}, q_k) = 0 \in T_{q_k}^* Q. \quad (\text{F.3})$$

In this picture, given two initial points (q_0, q_1) , Eq. (F.3) determines iteratively q_{k+1} from the two previous points (q_{k-1}, q_k) for $k \geq 1$.

For the case where Q is a Lie group G , in the spirit of the earlier trivialized expressions, instead of working with pairs (g_k, g_{k+1}) of consecutive points in a trajectory, one can chose to work with “pointing arrows”, pairs of the form *source-arrow* (g_k, h_k) pointing towards a *target* $g_k h_k = g_{k+1}$. With this perspective in mind, define the “trivialized” discrete Lagrangian and forces as follows

$$\bar{l}_k(g, h) := l_k(g, gh), \quad \bar{f}_k^\pm(g, h) := L_{\text{pr}_\pm(g, gh)}^* f_k^\pm(g, gh),$$

where pr_- and pr_+ are the source and target projection, respectively. After simple manipulation, together with the reconstruction equation $g_{k+1} = g_k h_k$, the Euler-Lagrange equation (F.3) reads

$$L_{g_k}^* \partial_g \bar{l}_k - R_{h_k}^* \partial_h \bar{l}_k + L_{h_{k-1}}^* \partial_h \bar{l}_{k-1} + \bar{f}_k^- + \bar{f}_{k-1}^+ = 0 \in \mathfrak{g}^*, \quad (\text{F.4})$$

where $\partial_m \bar{l}_k$ is a shorthand notation for $\partial_m \bar{l}_k(g_k, h_k)$ with $m = g, h$, and similarly for \bar{f}_k^\pm .

References

- P.-A. Absil, R. Mahony, and R. Sepulchre. *Optimization algorithms on matrix manifolds*. Princeton University Press, Princeton, NJ, 2008. ISBN 978-0-691-13298-3. doi: 10.1515/9781400830244. URL <https://doi.org/10.1515/9781400830244>. With a foreword by Paul Van Dooren.
- R. Bernardini and R. Rinaldo. Demystifying Lie Group Methods for Signal Processing: A Tutorial. *IEEE Signal Processing Magazine*, 38(2):45–64, 2021. doi: 10.1109/MSP.2020.3023540.
- Sergio Blanes and Fernando Casas. *A concise introduction to geometric numerical integration*. Monographs and Research Notes in Mathematics. CRC Press, Boca Raton, FL, 2016. ISBN 978-1-4822-6342-8.
- Nawaf Bou-Rabee and Jerrold E. Marsden. Hamilton-Pontryagin integrators on Lie groups. I. Introduction and structure-preserving properties. *Found. Comput. Math.*, 9(2):197–219, 2009. ISSN 1615-3375. doi: 10.1007/s10208-008-9030-4. URL <https://doi.org/10.1007/s10208-008-9030-4>.
- Cédric M. Campos, Alejandro Mahillo, and David Martín de Diego. Discrete variational calculus for accelerated optimization. *J. Mach. Learn. Res.*, 24:Paper No. [25], 33, 2023. ISSN 1532-4435,1533-7928. URL <https://jmlr.org/papers/v24/21-1323.html>.
- J. R. Cardoso and F. Silva Leite. The Moser-Veselov equation. *Linear Algebra Appl.*, 360:237–248, 2003. ISSN 0024-3795,1873-1856. doi: 10.1016/S0024-3795(02)00450-0. URL [https://doi.org/10.1016/S0024-3795\(02\)00450-0](https://doi.org/10.1016/S0024-3795(02)00450-0).
- Valentin Duruisseaux and Melvin Leok. A variational formulation of accelerated optimization on Riemannian manifolds. *SIAM J. Math. Data Sci.*, 4(2):649–674, 2022. ISSN 2577-0187. doi: 10.1137/21M1395648. URL <https://doi.org/10.1137/21M1395648>.
- Valentin Duruisseaux and Melvin Leok. Practical perspectives on symplectic accelerated optimization. *Optim. Methods Softw.*, 38(6):1230–1268, 2023a. ISSN 1055-6788,1029-4937. doi: 10.1080/10556788.2023.2214837. URL <https://doi.org/10.1080/10556788.2023.2214837>.
- Valentin Duruisseaux and Melvin Leok. Practical perspectives on symplectic accelerated optimization. *Optim. Methods Softw.*, 38(6):1230–1268, 2023b. ISSN 1055-6788,1029-4937. doi: 10.1080/10556788.2023.2214837. URL <https://doi.org/10.1080/10556788.2023.2214837>.
- E. Hairer, C. Lubich, and G. Wanner. *Geometric numerical integration*, volume 31 of *Springer Series in Computational Mathematics*. Springer, Heidelberg, 2010. ISBN 978-3-642-05157-9. Structure-preserving algorithms for ordinary differential equations, Reprint of the second (2006) edition.
- J. E. Marsden and M. West. Discrete mechanics and variational integrators. *Acta Numer.*, 10:357–514, 2001. ISSN 0962-4929. doi: 10.1017/S096249290100006X. URL <http://dx.doi.org/10.1017/S096249290100006X>.

- Yu. E. Nesterov. A method for solving the convex programming problem with convergence rate $O(1/k^2)$. *Dokl. Akad. Nauk SSSR*, 269(3):543–547, 1983. ISSN 0002-3264.
- Yurii Nesterov. *Introductory lectures on convex optimization*, volume 87 of *Applied Optimization*. Kluwer Academic Publishers, Boston, MA, 2004. ISBN 1-4020-7553-7. doi: 10.1007/978-1-4419-8853-9. URL <https://doi.org/10.1007/978-1-4419-8853-9>. A basic course.
- Boris T. Polyak. Some methods of speeding up the convergence of iterative methods. *Ž. Vyčisl. Mat i Mat. Fiz.*, 4:791–803, 1964. ISSN 0044-4669.
- H. H. Rosenbrock. An automatic method for finding the greatest or least value of a function. *Comput. J.*, 3:175–184, 1960/61. ISSN 0010-4620. doi: 10.1093/comjnl/3.3.175. URL <https://doi.org/10.1093/comjnl/3.3.175>.
- J. M. Sanz-Serna and M. P. Calvo. *Numerical Hamiltonian problems*, volume 7 of *Applied Mathematics and Mathematical Computation*. Chapman & Hall, London, 1994. ISBN 0-412-54290-0.
- Weijie Su, Stephen Boyd, and Emmanuel J. Candès. A differential equation for modeling nesterov’s accelerated gradient method: Theory and insights. *Journal of Machine Learning Research*, 17(153):1–43, 2016. URL <http://jmlr.org/papers/v17/15-084.html>.
- Molei Tao and Tomoki Ohsawa. Variational optimization on lie groups, with examples of leading (generalized) eigenvalue problems. *Proceedings of Machine Learning Research*, 108, 2020. URL <https://par.nsf.gov/biblio/10279890>.
- Andre Wibisono, Ashia C. Wilson, and Michael I. Jordan. A variational perspective on accelerated methods in optimization. *Proc. Natl. Acad. Sci. USA*, 113(47):E7351–E7358, 2016. ISSN 0027-8424. doi: 10.1073/pnas.1614734113. URL <https://doi.org/10.1073/pnas.1614734113>.